Chinese Industry and Technology of Eco-environment
2025, VOL. 6, NO. 4, 5-12
DOI: 10.47297/wspciateWSP2633-772X01.20250604

Spatiotemporal Analysis and Driving Factors of Desertification in Babusha Forest Farm

Pengxu Yan, Yijie Cao, Hao Zhang, Wenmian Guo, Huawen Wang

College of Geography and Environmental Science, Northwest Normal University, Lanzhou Gansu, 730070, China

ABSTRACT

Land desertification is one of the most severe ecological challenges facing China, and it is particularly pronounced in the country's western regions. Therefore, it is crucial to select various desertification monitoring indicators for annual spatiotemporal analysis, to construct a composite ecological index, and to investigate the primary factors driving desertification. The research focuses on Babusha Forest Farm in Gulang County, a key national desertification monitoring location. We derive an integrated ecological index from three measures—vegetation coverage (FVC), desertification index (DI), and remote sensing ecological index (RSEI)—spanning 1986 to 2021. We correlate this index with net primary productivity (NPP) to analyze the spatiotemporal patterns of desertification, forecast future trends, and finally build a grey relational model incorporating cultivated land area, construction land area, precipitation, and temperature to identify the main drivers of desertification at the site. The results indicate that desertification at Babusha Forest Farm is continually improving. Combined land-use data demonstrate that increases in both cropland and grassland drive ecological recovery, with cropland expansion exerting the greatest impact. The correlation between the integrated ecological index and NPP confirms the index's strong utility and overall reliability as an indicator in desertification monitoring. The grey relational model linking the composite ecological index with cultivated land area, construction land area, precipitation, and temperature yields grey relational degrees of 0.7012 and 0.7238 for anthropogenic factors, versus 0.6653 and 0.6552 for natural factors, indicating that human activities are the principal drivers of desertification improvement at Babusha Forest Farm.

KEYWORDS

Desertification; Babusha forest farm; Monitoring indicators; Spatiotemporal variation analysis; Driving factors

1 Introduction

In recent years, China has witnessed a marked escalation in land desertification, triggering ecological crises including dust storms, smog, and the degradation of grasslands and woodlands, which have substantially impeded growth in the West and now extend effects into the country's central and eastern areas. This is not merely a regional environmental challenge but a pivotal issue for China's long-term stability and security. Effectively addressing land desertification remains an urgent task in the construction of China's ecological civilization. According to the Fifth National Survey on Desertification and Sandy Land, by its conclusion desertified land in China covered 2.6116 million km^2—over one-fifth of the national territory—with sandy land exceeding 1.7 million km^2 [1]. China's western regions are the primary areas of desertified and sandy lands, severely disrupting ecological balance and hindering sustainable development there. Babusha Forest Farm in Gulang County—situated 30 km northeast of Gulang town on the southern edge of the Tengger Desert—serves as a key geographic barrier against the desert's southward expansion. By focusing on Babusha Forest Farm, this research aims to deliver a representative desertification analysis with high reference value, offering a scientific basis for ecological management and economic planning in this region and nationwide.

Initially, desertification research relied heavily on Normalized Difference Vegetation Index (NDVI) for vegetation dynamics across scales. With advances in remote sensing, researchers have leveraged NDVI quantitatively to investigate factors influencing regional vegetation growth [2]. Many studies integrate NDVI and Fractional Vegetation Cover (FVC) to derive desertification indices over long monitoring periods, enabling spatiotemporal analyses of distribution patterns and evolutionary trends [3-4]. Net Primary Productivity (NPP) research is also well established; in desertified regions, studies focus on the impacts of climatic variables [5] and land-use types on NPP. However, relying solely on NDVI, FVC, or NPP for desertification monitoring addresses only individual aspects and thus has inherent limitations. Some researchers have adapted the Remote Sensing Ecological Index (RSEI), improving and applying it—for example, Firozjaei et al [6]. proposed the Land Surface Ecological Status Composition Index (LSESCI) to distinguish bare soil from degradation-affected land; others developed the Arid Remote Sensing Ecological Index (ARSEI), integrating greenness, humidity, salinity, heat, and land degradation metrics for drylands [7]. Yet these tailored indices suffer from limited universality and insufficient integrative capacity. Constructing integrated evaluation models can overcome these shortcomings. Xi Lei et al [8]. developed a comprehensive desertification risk index—based on 16 indicators across climate, human activity, and monitoring status—using combined subjective-objective entropy weighting, markedly improving risk assessment accuracy and practical utility. Nevertheless, these integrated models typically require extensive data inputs and entail cumbersome computational procedures. In summary, formulating a unified composite desertification index not only mitigates the shortcomings of single-indicator approaches and enhances overall judgment, but also streamlines decision-making and statistical analysis, thereby establishing a standard monitoring metric and facilitating cost-effective implementation. This paper analyzes domestic and international research, performs spatiotemporal analyses using multiple desertification metrics, and constructs a composite ecological index—integrating vegetation structure, function, and stress via FVC, Desertification Index (DI), and RSEI—to evaluate desertification. Finally, it investigates the driving factors in the study area, offering scientific basis for long-term rehabilitation assessments in arid zones and theoretical guidance for ecological management strategies in similar regions.

2 Overview of the study area

Babusha Forest Farm is situated in Gulang County, Wuwei City, Gansu Province, between 102° 57′E and 103° 50′E longitude and 37° 25′N and 37° 55′N latitude, encompassing the areas of Tumen Town, Yongfengtan Township, and Huanghuatan Township. It falls within a temperate arid climatic zone characterized by large diurnal temperature variations, scant precipitation, and high evapotranspiration rates. The mean annual temperature is approximately 6.6 °C, with an average annual precipitation of about 210 mm and an annual evaporation reaching 3000 mm [9], imposing constraints on vegetation growth and land utilization. The elevation is 1620 m above sea level. The terrain is aeolian in origin, featuring wind-eroded and deposited sandy landforms such as mobile dunes, fixed and semi-fixed dunes, and gently sand-covered plains. Vegetation is dominated by drought-resistant shrubs and herbaceous species—such as sea buckthorn, Nitraria tangutorum, and Elaeagnus angustifolia—which play key roles in sand stabilization, wind erosion reduction, and biodiversity enhancement. The soil is predominantly Calcic Gray Brown Soil, offering good water retention and aeration, but regional groundwater scarcity exacerbates water supply–demand conflicts. Over the last four decades, the vegetative cover has shown a marked increase.

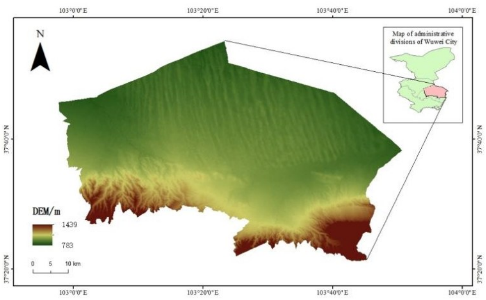

Figure 1 Study area overview map

3 Data Sources and Processing

3.1 Data sources

This research utilizes May–September Landsat 5 and Landsat 8 imagery (1986–2021) obtained via Google Earth Engine, with each scene featuring less than 10 % cloud coverage. The NPP dataset is derived from MOD17A3HGF V6 (2000–2021) at a 500 m resolution, representing the highest spatial detail and longest temporal coverage currently available. The study employs the Annual China Land Cover Dataset (CLCD) by Yang Jie and Huang Xin et al. (Wuhan University), which provides yearly land-cover maps for 1985–2021 at 30 m resolution and ~80 % classification accuracy [10]. Meteorological variables (temperature, precipitation, wind speed, etc.) are sourced from the monthly ERA5 aggregates (01/01/1986–02/01/2021) on the GEE platform.

3.2 Construction of individual indicators

(1) Fractional Vegetation Cover (FVC) denotes the percentage of the ground area covered by the vertical projection of vegetation, serving as a key quantitative metric of surface vegetation status and an indicator of the integrated effects of climate and land-use changes. Using GEE, we selected scenes with < 10 % cloud cover and computed FVC (1986–2021) via the pixel-binary model applied to the Normalized Difference Vegetation Index [11-13].

(2) As no reliable Landsat-based NPP algorithm exists, this study uses the MOD17A3HGF V6 product (2000–2021, 500 m resolution) as the most spatially detailed and temporally extensive NPP dataset available.

(3) The desertification index (DI) provides an effective quantitative measure of regional desertification severity. We construct DI using surface albedo and the Modified Soil-Adjusted Vegetation Index (MSAVI). Albedo quantifies surface exposure—higher in sandy areas—while MSAVI corrects for soil background to accurately represent sparse vegetation cover and sand - fixation capacity in arid zones. Their difference accentuates desertification dynamics through an antagonistic interplay between soil exposure and vegetation cover. This DI computation is physically compatible with traditional methods such as the NDVI – albedo feature - space approach [14] and aligns with the interactive processes between surface dynamics and vegetation feedback in arid regions.

$$DI = Albedo - SAVI$$

$$Albedo = 0.356BLUE + 0.130\mathrm{RED} + 0.373\mathrm{NIR} + 0.085\mathrm{SWIR1} + 0.072\mathrm{SWIR2} - 0.0018$$

$$MSAVI=\frac{1}{2}\times[2(NIR+1)-\sqrt[2]{(2NIR+1)^2-8(NIR-RED)}]$$

BLUE, RED, NIR, SWIR1, and SWIR2 denote the blue, red, near-infrared, shortwave-infrared 1, and shortwave-infrared 2 spectral bands, respectively.。

（4）The Remote Sensing Ecological Index (RSEI) is an ecological quality indicator derived via principal component transformation of four metrics: greenness (representing vegetation cover), humidity (reflecting moisture components), heat (denoting land surface temperature), and dryness (expressed by bare-soil and built-up indices). This index is simple to compute and entirely based on remote sensing data, yielding objective and consistent assessments of regional ecological quality; it has been widely applied to ecological quality evaluation and change analysis across various regions [15]. The formula is shown below::

$$RSEI=f\left(Greenness,Wetness,Dryness,Heat\right)$$

The four remote-sensing indices are the Normalized Difference Vegetation Index (NDVI), Wetness (WET), the Normalized Difference Soil Index (NDBSI), and Land Surface Temperature (LST), which correspond to greenness, wetness, dryness, and heat, respectively.

3.3 Methodology for computing the integrated ecological index

The Entropy Method is an information-theory – based approach for determining weights. In this study, the three indicators FVC, DI, and RSEI are standardized; their proportions are computed and entropy values calculated, from which the weight of each indicator is derived. Then, by applying linear weighting, the normalized values of FVC, DI, and RSEI are multiplied by their corresponding weights to construct the CEI. A higher CEI indicates stronger ecological resilience at Babusha Forest Farm.

（1）Pearson Correlation Coefficient Analysis: The Pearson correlation coefficient is a statistical measure used to quantify the strength and direction of the linear relationship between two variables. It is typically denoted by the symbol r and ranges in value from −1 to +1. Typically, r values between 0 and 0.2 denote negligible or very weak correlation; 0.2–0.4 weak; 0.4–0.6 moderate; 0.6–0.8 strong; and 0.8–1 very strong correlation.

（2）Grey Relational Analysis: Grey Relational Analysis (GRA) is primarily employed to analyze and quantify the degree of association among multiple factors. We assign the composite ecological index to the reference series X_0, and treat each natural and human-induced factor as comparison series X_1,X_2, ⋯ , Xi(i=1,2 , ⋯ , n)

$$\zeta_i(k)=\frac{\min\limits_i\min\limits_k\left|x_0(k)-x_i(k)\right|+\rho\cdot\max\limits_i\max\limits_k\left|x_0(k)-x_i(k)\right|}{\left|x_0(k)-x_i(k)\right|+\rho\cdot\max\limits_i\max\limits_k\left|x_0(k)-x_i(k)\right|}$$

In the equation, ρ denotes represents the resolution coefficient, which is commonly set to 0.5; $|X_0(k)-X_i(k)|$ denotes the absolute difference between the value of factor X_i and the composite ecological index X_0 in year k; min_{i,k}$|X_0(k)-X_i(k)|$ refers to the smallest absolute difference across all factors and years; max_{i, k}$|X_0(k)-X_i(k)|$ refers to the largest. The average of the annual grey relational coefficients over multiple years is taken as the relational degree r_i for each factor, as given by:

$$\Gamma_i=\frac{1}{n}\sum_{k=1}^{n}\zeta_{xi}(k)$$

Here, n denotes the number of years. Finally, in accordance with the principles of comprehensive grey relational analysis, the main factors influencing desertification at Babusha Forest Farm are investigated [16].

4 Results and analysis

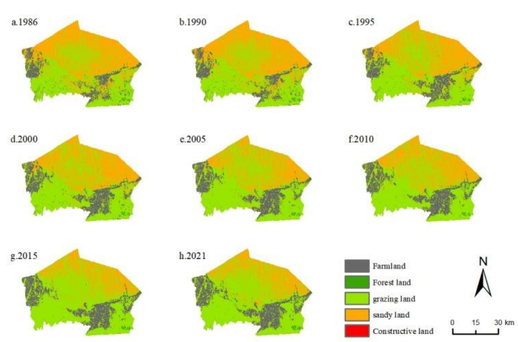

Figure 2 Spatiotemporal variation of land use in babusha forest farm, 1986–2021

4.1 Spatiotemporal analysis of land use at babusha forest farm (1986–2021)

As shown in Figure 2, during the study period Babusha Forest Farm ' s land use was dominated by grassland (low-density grassland) and desert areas, with comparatively small proportions of forest and built-up land. Table 1 indicates that between 1986 and 2021 the area under desertified land at Babusha Forest Farm progressively decreased, whereas grassland and farmland expanded, the former rising most markedly from 46.18 % to 60.24 %. In terms of spatial distribution, cropland was primarily located in the farm's northwest and southern sectors; landscape fragmentation diminished over time, resulting in pronounced spatial clustering. Desert areas were chiefly located in the central and northern parts of the farm, with their spatial extent continuously contracting—from 42.7 % down to 22.18 %—until by the end of the study period the central desert zone had nearly vanished. Consequently, over the past thirty years Babusha Forest Farm has experienced marked environmental improvement and achieved significant sand - control outcomes. Nonetheless, it should be noted that given the study area's arid and water - scarce conditions, the expansion of agricultural land poses potential ecological risks to the forest farm.

Table 1 Areas of land-use categories at babusha forest farm (1986–2021)

		Cropland	Forest land	Grassland	Desert	Construction land
1986	Area (km^2)	313.29	6.24	1326.04	1226.16	0.03
	Proportion	10.91%	0.22%	46.18%	42.70%	0.001%
1990	Area (km^2)	296.92	6.25	1347.77	1220.80	0.03
	Proportion	10.34%	0.22%	46.93%	42.51%	0.001%
1995	Area (km^2)	363.73	6.68	1475.65	1025.70	0.03
	Proportion	12.67%	0.23%	51.38%	35.72%	0.001%
2000	Area (km^2)	418.90	6.75	1489.01	957.10	0.04
	Proportion	14.59%	0.24%	51.85%	33.33%	0.002%
2005	Area (km^2)	440.03	6.99	1659.04	765.66	0.09
	Proportion	15.32%	0.24%	57.77%	26.66%	0.003%
2010	Area (km^2)	457.95	7.01	1599.36	807.36	0.13
	Proportion	15.95%	0.24%	55.69%	28.11%	0.01%
2015	Area (km^2)	475.06	7.84	1788.54	600.17	0.20
	Proportion	16.54%	0.27%	62.28%	20.90%	0.01%
2021	Area (km^2)	496.20	8.13	1730.01	637.08	0.27
	Proportion	17.28%	0.28%	60.24%	22.18%	0.01%

4.2 Time-series analysis of FVC, DI, and RSEI

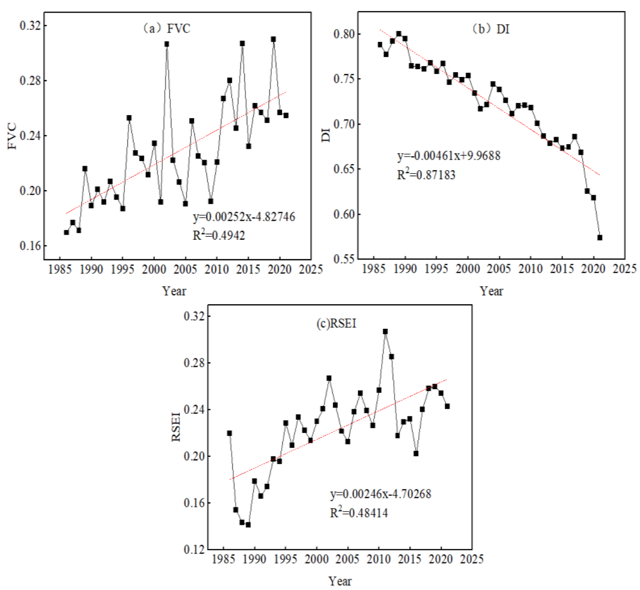

Figure 3 Interannual variations of FVC, DI, and RSEI at babusha forest farm

Figure 3 shows that over the 36-year period from 1985 to 2021, the overall ecological condition of the study area has markedly improved, with notable success in desertification control. The FVC exhibited a fluctuating upward trend at a rate of 0.0252 per decade; it reached a maximum of 0.3105 in 2019 and a minimum of 0.1698 in 1986, with the most rapid increase occurring between 2000 and 2005. However, the series remained relatively unstable, oscillating between 0.15 and 0.35. The DI displayed a steady decline at a rate of 0.0461 per decade, with limited fluctuation between 0.55 and 0.80. Specifically, DI peaked at 0.8002 in 1989 and reached its minimum of 0.5737 in 2021, with the steepest decrease occurring between 2015 and 2021. The RSEI rose initially, then declined before stabilizing, yet overall it increased at 0.0246 per decade, fluctuating between 0.12 and 0.32; it recorded a minimum of 0.1411 in 1989 and a maximum of 0.3069 in 2011. In summary, these trends indicate that vegetation cover at Babusha Forest Farm is continually improving and desert areas are contracting; notably, after 2015, the rate of ecological recovery intensified before leveling off into a dynamic equilibrium.

4.3 Spatial variation analysis of FVC, DI, and RSEI

Between 1986 and 2021, the multi-year mean distributions and temporal trends of FVC, DI, and RSEI at Babusha Forest Farm exhibited pronounced spatial heterogeneity. As shown in Figure 4, the long-term average FVC increases in a gradient from the periphery toward the center: low-coverage areas (<0.11) occupy 41 % of the region (primarily in the north), medium coverage (0.11–0.48) covers 43 % (centrally), and high coverage (0.48–1) accounts for only 16 %, located in the west and southeast. The DI exhibits low values in the northwest and southeast flanks and higher values in the northeast, southwest, and central areas: regions with DI < 0.64 cover 20 % (west and southeast), whereas DI > 0.74 spans 63 % of the area (north and southwest). The mean spatial distribution of RSEI closely mirrors that of FVC. Comparatively, the inverse relationship between the mean DI pattern and those of FVC/RSEI corroborates the validity of the DI computation.

Integrated with Figure 2 land-use data, the results indicate a sustained improvement in vegetation cover over the study period, with ecological enhancement closely linked to cropland and forest expansion, while grassland contributions remain modest. Areas of mild desertification coincide with cropland and forests, whereas regions of moderate desertification correspond spatially to grassland extents. High-value RSEI zones strongly correlate with cropland and forest areas, and mid-value zones with grasslands; trends from 2010–2015 reveal that cropland expansion contributed more to ecological improvement than grassland expansion. Furthermore, changes in mid-value RSEI zones from 2015–2021, alongside DI and land-use shifts, suggest that while low-coverage grasslands effectively stabilize dunes, their impact on overall ecological quality enhancement remains limited.

According to Figure 5, spatial trends in FVC are heterogeneous: areas with marked declines are scattered, whereas the sparsely vegetated north exhibits improvement or stability. DI trends negatively mirror those of FVC: formerly high-desertification areas in the north and south continued to worsen (weak increase 34 %, significant increase 2 %), while stable (39 %), slight decrease (17 %), and marked decrease (8 %) zones together underscore that higher vegetation effectively curbs desertification. RSEI trends exhibit general congruence with FVC, albeit with variations in the spatial extents. Areas with significant and slight RSEI declines are scattered (2 % and 12 %, mainly north and south), likely due to desert advance and vegetation loss; in contrast, southeast and west show stable (54 %), slight increase (23 %), and marked increase (9 %) zones, reflecting the patterns seen in FVC and DI.

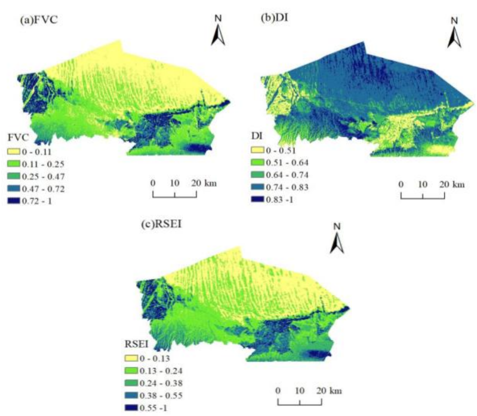

Figure 4 Multi-year mean spatial distribution patterns of FVC, DI, and RSEI at babusha forest farm

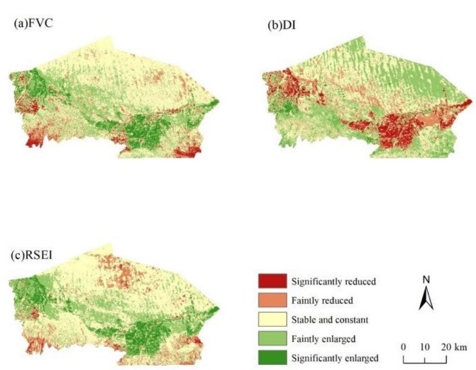

Figure 5 Spatial distribution of trend changes for FVC, DI, and RSEI at babusha forest farm

4.4 Spatiotemporal analysis of the composite ecological index

As shown in Figure 6, the CEI's long-term average distribution and its trend exhibit pronounced spatial heterogeneity, with interannual variations displaying an overall fluctuating upward trajectory. In the multi-year mean spatial distribution (Fig. 6a), there is a clear gradient of low values in the north to high values in the south. Northern areas mainly exhibit low CEI values (< 0.38), covering 42 % of the region, but medium values (0.38–0.50) also occur; in conjunction with land-use patterns, this likely reflects the rapid expansion of grasslands within desert areas in the north. The southern sector predominantly features medium and high CEI values (> 0.50). Medium and high value areas account for 40 % and 18 % of the total, respectively; notably, high-value zones coincide closely with cropland areas, indicating that cropland expansion has played a key role in increasing the CEI.

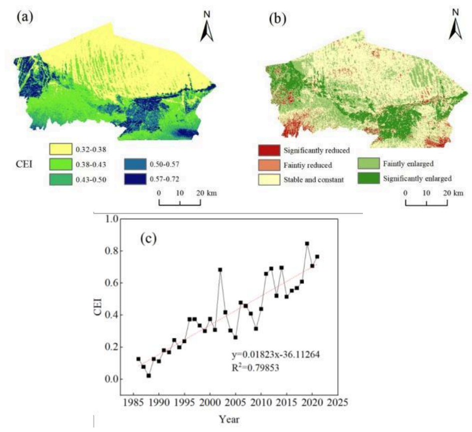

Figure 6 Multi-year mean spatial distribution of the composite ecological index (a), spatial pattern of its trend changes (b), and interannual variations (c) at babusha forest farm

In terms of trend patterns, areas exhibiting a decrease in CEI are scattered but predominantly located in the southwest and southeast, with regions of significant and slight decreases accounting for 3% and 7%, respectively. In the central region—particularly cropland areas—the CEI shows slight and pronounced increases, covering 26% and 14% of the area, respectively. Conversely, the northern desert and grassland zones as well as parts of the southern mountainous areas exhibit stable CEI values, representing 50% of the study area. In terms of interannual change, the CEI increases rapidly at 0.1823 per decade, peaking at 0.84 in 2019 and bottoming at 0.02 in 1988, indicating a rapid and significant growth effect. The coefficient of determination (R^2) for the interannual trend is 0.79853, indicating that the linear regression model fits the data well, with strong explanatory power and high predictive accuracy.

4.5 Correlation analysis of the composite ecological index and NPP and future prediction of desertification at babusha forest farm

Using linear regression, we analyzed the CEI and NPP values at Babusha Forest Farm from 2000 to 2021; the resulting fit is shown in Figure 7. The regression prediction, combined with Pearson correlation analysis, produces a correlation coefficient of R = 0.91 between CEI and NPP. According to standard interpretation, an R value between 0.8 and 1.0 indicates a very strong correlation. This result demonstrates a significant linear relationship between CEI and NPP, consistent with ecological theory that higher productivity enhances ecosystem services and resilience—underscoring both the pivotal role of vegetation productivity in environmental improvement and the necessity of steadfast implementation of afforestation and other restoration policies. Moreover, since NPP serves as a common metric that both indicates desertification status and quantifies the influence of various drivers [17], the very strong positive correlation with CEI attests to the index's scientific validity and utility, supporting its use as a key desertification-monitoring indicator.

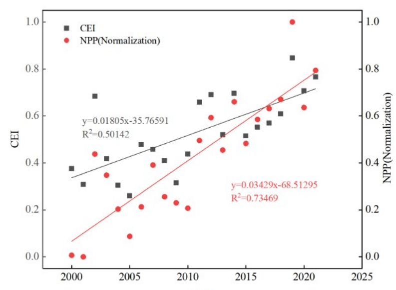

Figure 7 Linear regression between normalized NPP and composite ecological index (2000–2021) at babusha forest farm

This provides a forecast of future desertification at Babusha Forest Farm based on the composite ecological index. As shown in Figure 7, the CEI increased at a rate of 0.1805 per decade from 2000 to 2021. If this linear trend persists through 2030, the CEI would accumulate a gain exceeding 0.15 (relative to 2021), indicating continued suppression of desertification. Nevertheless, 26.53% of the variance remains unexplained, suggesting that external disturbances—such as changes in human activities or natural conditions—could affect predictive accuracy.

4.6 Investigation of driving factors using grey relational analysis

In the spatial analysis of individual desertification metrics and the composite ecological index—integrated with land-use data—it was found that grassland expansion contributes less to ecological restoration than cropland expansion and is constrained by both natural and anthropogenic factors, rendering it unsuitable as a standalone driver in the primary factor assessment. Therefore, this study constructs a grey relational model using cropland area and construction land area (representing anthropogenic influences) alongside temperature and precipitation (representing natural influences) as comparison sequences.

We treated temperature, precipitation, cropland extent, and construction land area as subordinate series and the composite ecological index as the master series. Using quinquennial intervals, we calculated each factor's grey relational coefficient and overall grey relational degree relative to the master series. As shown in Table 2, the grey relational degrees for anthropogenic variables substantially exceed those for natural variables, indicating that human activities are the principal drivers of desertification improvement at Babusha Forest Farm.

Table 2 Grey relational coefficients and degrees for natural and anthropogenic factors

Year	Temperature	Precipitation	Cropland Area	Construction Land Area
1986	1.0000	1.0000	1.0000	1.0000
1990	0.9110	0.9579	0.9786	0.9599
1995	0.7550	0.7440	0.7841	0.7480
2000	0.5787	0.5916	0.6136	0.6131
2005	0.7296	0.6557	0.7971	0.7380
2010	0.5253	0.5081	0.5648	0.7538
2015	0.4734	0.4506	0.5037	0.5044
2021	0.3496	0.3333	0.3677	0.4730
Grey Relational Degree(γ)	0.6653	0.6552	0.7012	0.7238

5 Conclusion and discussion

This study elucidates the spatiotemporal evolution patterns of desertification at Babusha Forest Farm from 1986 to 2021 and uncovers its driving mechanisms. The results indicate a marked reversal of desertification, with desert area reduced by nearly 50%, and FVC and the composite ecological index increasing at rates of 0.0252 and 0.1805 per decade, respectively. This improvement is closely linked to land-use transformation: cropland expanded to 496.20 km^2 (up 58.4%), and grassland to 1730.01 km^2 (up 30.5%), together enhancing sand fixation and carbon sequestration to jointly curb desertification. Notably, cropland expansion contributed most significantly to ecological enhancement, its spatial distribution closely matching high-CEI zones, indicating that agricultural intensification not only boosted productivity but also improved local hydrology via microtopographic modifications, fostering a positive ecological cycle. The grey relational model quantified driver strengths: anthropogenic factors (changes in cropland and built-up area) showed relational degrees of 0.7012 and 0.7238, far exceeding those of natural factors (precipitation and temperature, 0.6552 and 0.6653), confirming the central role of initiatives such as the "Three-North Shelterbelt" program, reforestation policies, and agricultural innovations. Moreover, the very strong positive correlation between the CEI and NPP ($R=0.91$) indicates that vegetation recovery is not only a hallmark of desertification control but also a key pathway for enhancing ecosystem services, offering empirical support for ecological restoration in arid regions worldwide.

This work innovatively developed a multidimensional CEI integrating vegetation structure, function, and stress, overcoming limitations of single-indicator analyses in capturing spatiotemporal heterogeneity, and revealed the nonlinear coupling between natural and anthropogenic factors via grey relational modeling. However, methodological refinements remain possible: entropy-based weighting may cause redundancy among greenness metrics (e.g., FVC and NDVI within RSEI), so future work could integrate PCA or similar approaches to optimize weight allocation. Additionally, while cropland expansion has driven short-term ecological gains, it may exacerbate water scarcity over the long term, necessitating dynamic remote sensing and field surveys to assess sustainability. Future research should examine the synergistic effects of precipitation and temperature under climate change and explore interactions between rural livelihood transitions and ecological policies to inform coordinated "human–land–water" management. Overall, this research offers a scientific paradigm for ecological restoration and green development in arid zones, with significant implications for desertification management in comparable regions worldwide.

Funding

Northwest Normal University 2025 College Students Innovation and Entrepreneurship ability improvement plan"2025+Spatiotemporal Analysis and Driving Factors of Desertification in Babusha Forest Farm"(NO: CXCYKT2025188)

References

[1] Tu Z, Li M, Sun T. Results and Analysis of the Fifth National Desertification and Sandy Land Monitoring. Journal of Forest Resource Management. 2016(01):1–5, 13.
[2] Sur K, Dave R, Prakash CH. Spatio-temporal Changes in NDVI and Rainfall over Western Rajasthan and Gujarat Region of India. Journal of Agrometeorology. 2018,20(3):189–195.
[3] Li Z, Liu H, Bai Y, Han B, Miao J, Du D, Xu D. Spatiotemporal Dynamic Monitoring of Desertification in Kangbao County, Zhangjiakou, Based on the Albedo–NDVI Feature Space. Acta Geologica Sinica. 2023;45(6):1–10.
[4] Sun S, Cao X, Xiao J, Sun W, Zhu C. Desertification Monitoring in the Qaidam Basin Based on the NDVI – Albedo Feature Space. Arid Meteorology. 2023;41(4):560–569.
[5] Liu Y, Yao X, Li Z, Hu J. Effects of Climate Change and Land-Use/Cover Change on Vegetation Net Primary Productivity in the Hexi Corridor. Research of Arid Regions. 2024;41(1):169–180.
[6] Karimi Firozjaei M, Fathololoumi S, Kiavarz M, Biswas A, Homaee M, Alavipanah SK. Land Surface Ecological Status Composition Index (LSESCI): A Novel Remote Sensing–Based Technique for Modeling Land Surface Ecological Status. Ecological Indicators. 2021;123:107375.
[7] Wang J, Ma J, Xie F, Xu X. Enhancement of the Remote Sensing Ecological Index in Arid Regions: A Case Study of the Ulan Buh Desert. Chinese Journal of Applied Ecology. 2020;31(11):3795–3804.
[8] Xi L, Feng Y, Qi Z, et al. Desertification Risk Assessment of the Tarim Basin Based on a Composite Evaluation Index. Acta Ecologica Sinica. 2025; 45(3):1126–1136. doi:10.20103/j.stxb.202308271844
[9] Hu X, Li X, Wang N. Spatiotemporal Evolution Analysis of Vegetation Cover in the Sand Control Zone of Babusha Forest Farm. Geospatial Information. 2022;20(1):66–69, 8.
[10] Yang J, Huang X. The 30 m Annual Land Cover Dataset and Its Dynamics in China from 1990 to 2019. Earth System Science Data. 2021;13(8): 3907–3925.
[11] Hao X, Zhang Z, Zheng H, Gao N. Spatiotemporal Variation Characteristics and Driving Factor Detection of Vegetation Cover in the Northern Tianshan Economic Belt. China Environmental Science. 2023;43(10):1–12.
[12] Fang H, Zhang Y, He Y, Li Z, Fan G, Xu D, Zhang C, He Z. Spatiotemporal Variation and Driving Factors of Vegetation Ecological Quality in Zhejiang Province. Remote Sensing of Natural Resources. 2023;35(2):245–254.
[13] Zhao A, Tian X. Spatiotemporal Evolution and Influencing Factors of Vegetation Cover on the Loess Plateau (1986–2021) Based on the GEE Platform. Journal of Ecology and Environment. 2022;31(11):2124–2133.
[14] Zeng Y, Xiang N, Feng Z, et al. Study on the Albedo – NDVI Feature Space and Remote Sensing Monitoring Index for Desertification. Geographical Sciences. 2006;(01):75–81.
[15] Xu H. Remote Sensing Evaluation Indices for Regional Ecological and Environmental Change. China Environmental Science. 2013;33(5):889 –897.
[16] Cheng X, Zhang Q, Lan F, Li Y, Han Y, Zhang L, Yang Y, Wang X. Dynamics and Driving Factors of Grassland Desertification in the Hexi Corridor. Journal of Desert Research. 2022;42(6):134–141.
[17] Xu D, Tong H, Li C, et al. A System Dynamics Model of Desertification Coupling Natural and Human Factors. Journal of Desert Research. 2015; 35(2):267–275.